Eur. J. Wood Prod.
DOI 10.1007/s00107-016-1124-0

ORIGINAL

Deflections in sawn timber beams with stochastic properties

Diego A. García[1,2,3] · **Marta B. Rosales**[1,3]

Received: 24 June 2015

Abstract A stochastic model is proposed to study the behavior of structural sawn beams of Argentinean *Eucalyptus grandis* with the aim of improving the predictability of the elastic deformations. The enhancement of the mid-span deflection calculation is based on a probabilistic model of the Modulus of Elasticity (MOE) and the representation of its lengthwise variability through a random field. The standard model that uses a MOE variable assumed random from piece to piece but deterministic (constant) within each piece is obtained as a particular case. In order to obtain a statistical representation of the MOE, the Principle of Maximum Entropy (PME) is employed. Experimental data obtained from bending tests are employed to find the parameters of the derived Probability Density Function (PDF). The PDF of the mid-span deformations is numerically obtained through the Stochastic Finite Element Method (SFEM) and Monte Carlo Simulations (MCS). Numerical results are validated with experimental values. Deflections of structural sized beams under usual loads are obtained. Finally, the stochastic model is used to compare with the serviceability requirements established in the Argentinean design code. It is shown that the structural performance of timber beams is found through a more realistic material approach.

✉ Diego A. García
garciadiego@fio.unam.edu.ar

[1] Department of Engineering, Universidad Nacional del Sur, Av. Alem 1253, 8000 Bahía Blanca, Argentina

[2] Department of Civil Engineering, Universidad Nacional de Misiones, Juan Manuel de Rosas 325, 3360 Oberá, Argentina

[3] CONICET, Buenos Aires, Argentina

1 Introduction

Timber as a construction material exhibits important variability in its mechanical properties. Thus, the analysis of the structural behavior of timber beams requires the inclusion of these variabilities in order to obtain significant results. Their performance should usually satisfy two main requirements. One is strength, usually expressed in terms of the load bearing capacity. The other requirement is serviceability, which refers to the ability of the structural system to perform satisfactorily under normal use. For this reason, serviceability is very important in the structural design. Design rules give recommendations for limits of instantaneous and final deformations which can be used in the absence of more precise information. A linear relationship between the total and the instantaneous deformations is usually assumed by the design rules included in the codes. Instantaneous deflection can be obtained by means of the standard solution based on elementary beam theory considering the MOE value constant throughout the structural member.

The timber species studied in this work is the Argentinean *Eucalyptus grandis*. A simple method for visually strength grading of this sawn timber has been developed by Piter et al. (2004a). In accordance with their results, it is possible to assign a grade of good quality Argentinean *Eucalyptus grandis* to the strength classes C30, C24 and C18 (from highest to lower quality) of the international system established in EN 338 (2009). As reported by Piter, the presence of pith and knots reduces significantly the strength and the stiffness of the timber. These features are also considered the most important visual characteristics for the strength grading of this material by the Argentinean standard IRAM 9662-2 (2006). The basis for the machine strength grading of this species was reported in Piter et al.

Published online: 14 November 2016

(2004b). However, no method for machine strength grading was adopted by this standard.

Due to its natural origin, structural timber is characterized by considerable lengthwise variability of its mechanical properties. However, these properties are usually treated as random variables and their spatial variability is not explicitly taken into account in design practice (i.e. they are considered constant along the length). The designer uses the properties established by the codes which are then applied to the calculation of the whole piece without considering that the defects and properties (within the established limits of the strength grading) vary along the length of the same piece. Growth defects such as knots are the main source of the lengthwise variability of the bending strength and stiffness in sawn beams. It is apparent that a stochastic approach that accounts for this effect becomes necessary in order to attain a more realistic structural model.

The stochastic approaches employed for the modeling of the timber mechanical properties are derived from the probabilistic theories of random variables and stochastic processes. These methods allow the simulation of the timber mechanical properties with the aim of performing the structural analysis. Random process approaches have been employed in order to simulate the lengthwise variability of the timber mechanical properties. As is mentioned in Kandler et al. (2015a), these approaches can be divided into Discrete Parameter Space Models (DPSM) and Continuous Parameter Space Models (CPSM). In the first group, timber elements are divided in segments of equal size and a single stiffness value is assigned to each segment. The second group can be divided into two subgroups: the Weak Zone Models (WZM) in which the location of the timber defects can vary randomly and another group that accounts for Continuous Stiffness Profiles (CSPM). Regarding the DPSM, one of the first studies was presented by Kline et al. (1986). In it, the MOE variability is modeled with a second-order Markov model. This method is applied in order to generate serially correlated MOEs along segments for a piece of lumber. Czmoch (1998) assumed the MOE variation as a stationary Gaussian random field simulated through the Nataf transformation (Der Kiureghian and Liu 1986) and the mid-span deflection was found through the Finite Element Method (FEM). Despite the fact that a continuous method was employed to simulate the random field, the discretization technique of the random process, the midpoint method (Der Kiureghian and Ke 1988), allows to classify it in the group of DPSM. In Lam and Varoğlu (1991), a model to simulate the lengthwise variation of the tensile strength was presented. These are some of the many works that employ the DPSM. The WZM are frequently intended to model bending and tensile strength, and to a lesser extent bending and tensile stiffness. Köhler (2007) models the lengthwise variability of the bending strength following the weak zone approach proposed by Isaksson (1999) for the bending moment capacity. Fink and Köhler (2014) report a model for the prediction of the local tensile strength and stiffness properties of knot clusters in structural timber. García et al. (2016) present a WZM of *Eucalyptus grandis* sawn beams, applied to the study of structural eigenproblems. In the weak zone model, the structural timber is represented as a composite of short weak zones connected by longer sections of clear wood. The WZM are also associated with the hierarchical models in which frequently two levels are distinguished, the first is the variability among members and the second one is the variability within each member due to the knot presence. This approach considers the equicorrelation of the random field, i.e. the values of the MOE along the timber member are equally correlated. Ditlevsen and Källsner (2005) report a hierarchical model which represents the lengthwise variability of the bending strength. Brandner and Schickofer (2015) use probabilistic models for the MOE and the shear modulus considering serial and parallel systems to represent timber elements. Finally, within the group of CSPM, Wang and Foschi (1992) carry out a reliability study in laminated beams in which the MOE is simulated by a stationary random process and the deflections are obtained through the FEM. Kandler et al. (2015b) study the influence of the longitudinal stiffness variability of wooden lamellas on the effective stiffness of Glued Laminated Timber (GLT) beams. The longitudinal stiffness profile of each lamella was obtained from the fiber angle information in combination with a micromechanical model for wood. The prediction of the effective GLT stiffness was carried out through a FEM model. Generally, hierarchical models employ a random field with an equicorrelation structure. In contrast, CSPM employs a correlation structure with Markov properties. An extensive literature review and discussion of both correlation approaches can be found in Brandner (2012).

The combination of stochastic approaches and the Finite Element Method (FEM) gives place to the Stochastic Finite Element Method (SFEM). In Der Kiureghian and Ke (1988), the SFEM is applied to perform structural reliability studies. Among other results, the authors studied several techniques for the simulation and discretization of the random field in order to obtain a good representation of the material properties variability. Ghanem and Spanos (1991) in their book related to SFEM, represent the random system parameters as second order stochastic processes defined by their mean and covariance functions. The Karhunen-Loève expansion is used to represent these processes in terms of a countable set of uncorrelated random

variables. This expansion is extensively employed in the simulation of Gaussian random fields. The non-Gaussian version of this method can be found in Mulani (2006). An alternative tool to simulate random fields is the Nataf transformation (e.g. Der Kiureghian and Liu 1986) applied to structural reliability studies under incomplete probability information of the random variables. If only marginal PDFs and correlation data are available, even for non-Normal random variables, the Nataf transformation can be applied to give a set of independent Normal random variables. Melchers (1999) deals with this transformation. The application of the methodology previously described together with the well-known Monte Carlo Simulation (MCS) approach, lead to a more realistic representation of mechanical systems. Frequently, the results of these models are employed to carry out reliability analyses in order to find the Probability of Failure (*PF*) of a system with stochastic properties (Melchers 1999).

The aim of the present work is to propose a stochastic model of the lengthwise variability of the MOE in timber sawn beams of Argentinean *Eucalyptus grandis* capable of improving the predictability of the mid-span deflection with respect to the traditional assumption of constant MOE along the beam span. The proposed stochastic model starts from a CSPM composed of a marginal probability distribution of the MOE and an adequate correlation structure. Unlike the reference works, the experimental information of the probability of the MOE is obtained from the third-point load bending tests. The construction of an adequate model starting from these experimental values supposes an advantage in comparison with models with a more precise material description and more expensive to develop. In order to state the stochastic model, in a first instance, the results obtained from two well-known theoretical beam models (*i.e.* Euler-Bernoulli and Timoshenko theories) with the timber properties applicable to each one (global and local MOE, respectively), are compared with experimental results. Then, after the most appropriate theory and material properties are selected, the PDF of the MOE is defined through the application of the Principle of Maximum Entropy (PME) proposed by Shannon (1948) and Jaynes (1957). Later, for the construction of a more realistic material model, the Nataf Transformation (NT) and the non-Gaussian Karhunen-Loève expansion (NGKL) are employed and their results obtained from MCS and the SFEM are compared. A validation of these numerical results with the experimental outcomes is carried out to study the applicability of the model. Then, the proposed stochastic model is employed to evaluate the mid-span deflection. Finally, a study regarding the serviceability performance is presented. The limits recommended by the Argentinean design rules (CIRSOC 601, 2013) for the instantaneous deflections are contrasted. The Monte Carlo Method (MCM) is employed for this analysis. The stochastic approach that takes into account the lengthwise variability of the MOE leads to a more precise prediction of the serviceability performance than the model with constant MOE along the beam span.

2 Materials and methods

The study of the mid-span deflection of a simply supported timber beam is presented herein. The mid-span deflection $v(L/2)$ can be evaluated after solving the well-known Euler–Bernoulli (E–B) equation as follows:

$$\frac{d^2}{dx^2}\left(e(x)i(x)\frac{d^2v(x)}{dx^2}\right) = f(x), \tag{1}$$

where $v(x)$ is the transverse displacement of the beam, $e(x)$ is the MOE, $i(x)$ is the second moment of area with respect to the z axis and $f(x)$ is the externally applied load. This expression is widely employed for the calculation of instantaneous deflections and its subsequent comparison with the limits established by the design rules. Despite that most of the results that will be presented in the work are based on the E–B beam theory, outcomes from the Timoshenko beam formulation will also be reported. The governing equations are:

$$\begin{cases} \dfrac{d}{dx}\left[g(x)a(x)k_s\left(\widehat{\psi}(x)+\dfrac{dv(x)}{dx}\right)\right]+f(x)=0 \\ \dfrac{d}{dx}\left(e(x)i(x)\dfrac{d\widehat{\psi}(x)}{dx}\right)-g(x)a(x)k_s\left(\widehat{\psi}(x)+\dfrac{dv(x)}{dx}\right)=0 \end{cases} \tag{2}$$

where $g(x)$ is the shear modulus, $a(x)$ is the beam cross section, k_s is the shear correction coefficient and $\widehat{\psi}(x)$ denotes the rotation about the z axis.

In the present work, the lengthwise variability of the MOE is represented by means of the random field $E(x)$. In what follows, capital letters denote random variables/processes. A deterministic value is assumed for the second moment of area i_0. The MOE modeled as a random variable E, and in consequence constant along the beam span, is then obtained as a particular case of the random (correlated) field. Equation (1) written with the random quantities $E(x)$ and $V(x)$ has the following expression:

$$\frac{d^2}{dx^2}\left(E(x)i_0\frac{d^2V(x)}{dx^2}\right) = f(x). \tag{3}$$

2.1 Finite elements discretization

Let us state the variational formulation prescribing a set of admissible functions ψ:

$$\int_0^L \left[\frac{\partial^2}{\partial x^2} \left(e(x) i(x) \frac{\partial^2 v(x,t)}{\partial x^2} \right) - f(x) \right] \phi(x) dx = 0 \quad \forall \phi \in \psi \tag{4}$$

For the pinned–pinned beam,

$$\psi = \{\phi : [0, L] \to \mathbb{R}, \phi \text{ is piecewise } C^2 \text{ and bounded}, \phi(0) = 0, \phi(L) = 0\}. \tag{5}$$

This formulation, together with the boundary conditions, conduces to the following form of the variational problem:

$$K(v, \phi) - F(\phi) = 0 \quad \forall \phi \in \psi \tag{6}$$

where $F(\phi)$ and $K(v, \phi)$ are the force and stiffness operators respectively, defined as follows:

$$K(v, \phi) = \int_0^L e(x) i(x) \frac{\partial^2 v(x,t)}{\partial x^2} \frac{\partial^2 \phi(x)}{\partial x^2} dx \quad \text{and}$$
$$F(\phi) = \int_0^L f(x) \phi(x) dx \tag{7}$$

Equation (6) is numerically approximated using the Galerkin Method. A N-dimensional subspace $\psi^N \subset \psi$ is defined and approximating functions $v^N \in \psi^N$ are searched for. The variational problem can be formulated as follows: Find $v^N \in \psi^N$ such that:

$$K(v^N, \phi) - F(\phi) = 0 \qquad \forall \phi \in \psi^N \tag{8}$$

Applying the standard finite element methodology (e.g. Bathe 1982) the variational form, (Eq. (8)) is discretized. Euler-Bernoulli beam elements with two nodes and two degrees of freedom per node (transverse displacement and rotation, respectively) are employed. *Hermitian* shape functions(n_i, n_j) for the spatial interpolation of the transverse deflection $v(x)$ in terms of nodal variables are considered. The components of the beam element stiffness matrix and the nodal force vector are obtained from:

$$K_{e,ij} = \int_0^{L_e} E(x) i_0 \frac{d^2 n_i(x)}{dx^2} \frac{d^2 n_j(x)}{dx^2} dx \quad \text{and}$$
$$F_{e,j} = \int_0^{L_e} f(x) n_j(x) dx. \tag{9}$$

After assembling the element stiffness matrices and vectors, the following matrix equation is obtained:

$$[K]\{d\} = \{F\}, \tag{10}$$

where $[K]$ is the $n \times n$ positive-definite global stiffness matrix, $\{d\}$ is the $n \times 1$ vector of global nodal displacements and $\{F\}$ is the $n \times 1$ vector of global nodal forces.

It is important to remark that in the first part of the study, the MOE is represented as a random field. Later, the particular case of a random variable is derived from it. Hence, in the following section, probabilistic tools to simulate a random field are introduced.

2.2 MOE lengthwise variability represented by a random field

A random field can be defined as a set of random variables which evolve as a function of a parameter, in this case the position x along the beam length. This set of random variables has a multidimensional PDF with a certain degree of correlation. In order to simulate the random field, it is necessary to define the characteristics of the set of random variables. In this subsection, the components of a multidimensional PDF will be presented.

2.2.1 Nataf transformation

The Nataf Transformation (NT) is employed in order to generate and simulate the MOE random field. It was introduced in the field of structural engineering by Der Kiureghian and Liu (1986). This method allows to build a multidimensional PDF that fits some prescribed marginal distributions $f_{X_i}(x_i)$ and some correlation matrix R:

$$f_X(x_1, \ldots, x_M) = \prod_{i=1}^{M} \frac{f_{X_i}(x_i)}{\varphi(\xi_i)} \varphi_M(\xi; R_0), \tag{11}$$

where φ_M and φ are the multidimensional and one-dimensional normal standard distributions, respectively. The correlation matrix R_0 is computed term by term by solving the following integral for ρ_{ij}:

$$\rho_{ij} = \int_{-\infty}^{\infty} \int_{-\infty}^{\infty} \left(\frac{x_i - \mu_{X_i}}{\sigma_{X_i}} \right) \left(\frac{x_j - \mu_{X_j}}{\sigma_{X_j}} \right) \varphi_2(\xi_i, \xi_j; \rho_{0ij}) d\xi_i d\xi_j, \tag{12}$$

where ρ_{ij} and ρ_{0ij} are the non-dimensional correlation matrix elements. In order to apply this method in this work, it is necessary to define the marginal PDF of the MOE and the correlation matrix of the random field. They are presented in the following subsections. For more details on this transformation, the interested reader is referred to Der Kiureghian and Liu (1986).

2.2.2 Non-Gaussian Karhunen–Loève expansion

In addition to the Nataf transformation and with the same purpose, the non-Gaussian Karhunen–Loève expansion (NGKL) is applied in order to simulate the MOE random field. The NGKL of the random field of the MOE has the following expression:

$$E(x,\theta) = \overline{E}(x) + \sum_{i=1}^{\infty} \sqrt{\lambda_i}\xi_i(\theta) f_i(x), \tag{13}$$

in which λ_i and $f_i(x)$ are the eigenvalues and eigenfunctions of the covariance function $C(x_1, x_2)$, respectively. By definition, $C(x_1, x_2)$ is bounded, symmetric and positive definite. Following the Mercer's Theorem, it has the following spectral decomposition:

$$C(x_1, x_2) = \sum_{i=1}^{\infty} \lambda_i f_i(x_1) f_i(x_2), \tag{14}$$

and its eigenvalues and eigenfunctions are the solution of the homogeneous Fredholm integral equation of the second kind given by

$$\int_D C(x_1, x_2) f_i(x_1) dx_1 = \lambda_i f_i(x_2). \tag{15}$$

The eigenfunctions form a complete orthogonal set. The parameter ξ_i is a set of uncorrelated random variables. If the random process is Gaussian, then $\xi_i(\theta)$ are zero mean uncorrelated Gaussian variables. Uncorrelated standard Normal variables are independent, so the question of independence does not arise in the Karhunen–Loève expansion of a Gaussian random process. Otherwise, in the case of non-Gaussian random variables, uncorrelated and independence are not equivalent. To obtain NGKL basis random variables $\xi_i(\theta)$ for a non-Gaussian process, the marginal density function should be available. Following the work of Mulani (2006), a non-linear transformation method is applied to obtain the NGKL basis random variables $\xi_i(\theta)$ of a non-Gaussian process. For the practical implementation, the series are approximated by a finite number of terms M, giving place to

$$E(x,\theta) = \overline{E}(x) + \sum_{i=1}^{M} \sqrt{\lambda_i}\xi_i(\theta) f_i(x). \tag{16}$$

2.3 Marginal PDF of the MOE

If a stochastic approach is applied to this problem, first a PDF should be chosen for the random variable. A statistical concept of entropy was introduced by Shannon (1948) and its maximization by Jaynes (1957). The Principle of Maximum Entropy (PME) states that, subjected to known constrains, the PDF which best represents the current state of knowledge is the one with largest entropy. The measure of uncertainties of a continuous random variable X is defined by the following expression

$$S(f_X) = -\int_D f_X(x) ln(f_X(x)) dx, \tag{17}$$

in which f_X stands for the PDF of the random variable X and D is its domain. The maximization of the entropy conduces to a optimization problem which can be solved through Lagrange multipliers.

In order to find the parameters of the marginal PDF of the MOE, experimental data presented by Piter (2003) are employed. These values were obtained by means of third-point loading bending tests, performed with 349 sawn beam samples of Argentinean *Eucalyptus grandis* of structural dimensions. The bending tests were carried out according to the standard EN 408 (1996). The worst defects of the beams were located in the constant bending moment zone, between the two concentrated loads and in the tensile region of the cross section. The sawn beams of the samples have the following dimensions (in mm): sample 1 (S1) 50 beams of 50 ×50 × 1000, sample 2 (S2) 50 beams of 50 × 75 × 1500, sample 3 (S3) 50 beams of 50 × 100 × 2000, sample 4 (S4) 50 beams of 50 × 150 × 3000 and sample 5 (S5) 149 beams of 100 × 25 × 500. Samples 1–4 were tested edgewise and sample 5, flatwise. The values of the MOE were calculated taking into account the shear deformation (global MOE E_{global}) in all the samples. Also, for S4, the local MOE (E_{local}) was obtained. This value of the MOE was calculated in the pure bending zone of the tested beams, free of shear deformations. The expressions to calculate the global and the local MOE are:

$$E_{global} = \frac{L^3(F_2 - F_1)}{4.7bh^3(w_{G2} - w_{G1})} \quad \text{and} \quad E_{local} = \frac{al_1^2(F_2 - F_1)}{16I(w_{L2} - w_{L1})} \tag{18}$$

where $(F_2 - F_1)$ is the load increment, $(w_{G2} - w_{G1})$ is the global mid-span deflection increment corresponding to the load increment, $(w_{L2} - w_{L1})$ is the local mid-span deflection increment measured in the constant moment region and corresponding to the same load increment, b is the width of the cross section, h the height of the cross section, a is the distance between one load and the nearest support, l_1 is the central gauge length of five times the height of the section and I is the second moment of area. The load increment is within the linear elastic range of the material. Values of the MOE experimentally obtained were corrected to a reference moisture content of 12% according to EN 384 (1996). In Table 1, the results of the bending test are shown.

The tested beams were visually strength graded according to the criterion adopted by the Argentinean standard IRAM 9662-2 (2006) (Table 2).

This code includes two strength classes (C1 and C2), while the third class (C3) is composed of pieces whose defects exceed the limits established for C1 and C2. The presence of pith and knots are considered the most important visual characteristics for the strength grading of this material. Each sample is composed of the following quantities and percentages of timber quality according to

Table 1 Summary of the results for mechanical properties corresponding to samples subjected to bending tests, Piter et al. (2004a)

Mechanical properties	Statistical values	S1 50 mm	S2 75 mm	S3 100 mm	S4 150 mm	S5 25 mm
f (N/mm^2)	Min	17.4	22.9	21.6	11.5	27.5
	Mean	42.4	53.6	43.9	40.3	62.1
	Max	80.3	115.1	65.2	67.2	111.4
	SD	12.3	16.8	10.2	13.1	15.8
E_g (N/mm^2)	Min	6800	7400	9000	8300	6100
	Mean	10,900	12,700	11,800	12,000	12,200
	Max	14,100	21,500	14,900	16,400	19,300
	SD	1860	2700	1560	1590	2440
ρ (kg/m^3)	Min	419	444	430	431	421
	Mean	533	567	527	513	564
	Max	705	1094	732	587	739
	SD	76	110	72	37	65

Bending strength (f), global MOE (E_g) and density (ρ)

Table 2 *Eucalyptus grandis* strength classes, according to the Argentinean standard IRAM 9662-2 (2006)

Strength class	Presence of pith	Knot ratio	Grain deviation
C1	No	K $\leq 1/3$	gd $< 1/12$
C2	No	$1/3 <$ K $\leq 2/3$	gd $< 1/9$
C3	Yes	$2/3 <$ K	$1/9 <$ gd

the visual grading (C1, C2, C3): S1 [8 (16%), 12 (24%), 22 (44%)], S2 [19 (38%), 13 (26%), 18 (36%)], S3 [9 (18%), 6 (12%), 35 (70%)], S4 [12 (24%), 3 (6%), 35 (70%)] and S5 [71 (48%), 29 (19%), 49 (33%)]. Then, a machine strength grading was also performed by Piter et al. (2004b), resulting in the following quantities and percentages: S1 [16 (32%), 16 (32%), 18 (36%)], S2 [29 (58%), 10 (20%), 11 (22%)], S3 [14 (28%), 9 (18 27 (54%)], S4 [18 (36%), 4 (8%), 28 (56%)] and S5 [82 (55%), 47 (31%), 20 (14%)]. The Argentinean standard IRAM 9662-2 (2006) only considers the visual strength grading.

Structural elements of this timber species subjected to bending usually present a nominal height ranging from 25 to 150 mm. The lowest height is typical for boards loaded on the wider face. Pieces with a height higher than 150 mm are not usually available because of the relatively small diameter of the stems which are normally obtained from short rotation plantation trees.

According to the American standard ASTM D 198 (2002), the third-point load bending test is representative of the usually assumed uniform load distribution on beams. When the loads are applied at the one-third points the moment distribution of the beam simulates that for loads uniformly distributed across the span to develop the bending moment of similar magnitude.

2.4 Correlation function of the MOE random field

The structure of the random field is described by means of the correlation function. Traditionally two structures of correlation have been employed in the references works regarding the lengthwise variability of mechanical timber properties. The first one is the correlation with distance dependence and the second is the equicorrelation model. In accordance with Continuous Stiffness Profiles Models (CSPM), which frequently employ correlation structures with Markov properties, an exponential correlation function proposed by Czmoch (1998) is assumed. It is based on experimental test carried out on pine-spruce beams grade K24 according to the Swedish standard SBN 1980 (1981) and it writes

$$\rho_{ij} = exp\left(-2\frac{\left|x_c^{(j)} - x_c^{(i)}\right|}{d}\right), \tag{19}$$

where d is the correlation length which measures the decay of the correlation. Here, the values considered for the correlation length of the MOE random field are d =1.34 m (d_1) and $d \to \infty$ (d_∞). When $d \to \infty$, the random field becomes fully correlated and it can be interpreted as a random variable in the limit. It represents a beam with homogeneous stochastic MOE. This case is used in the design practice and in reliability studies.

Czmoch (1998) found experimentally that the correlation length of the MOE for pine-spruce beams, is approximately 1.4 m for the serviceability load level, and around 0.7 m for a load level close to the load carrying capacity. These values of correlation length were determined in beams with dimensions and load levels similar to the ones employed in the following sections of the present work.

The *Eucalyptus grandis* cultivated in the Mesopotamian provinces of Argentina has a very high MOE/density ratio more similar to that adopted by European standards for poplar and coniferous than the corresponding one to deciduous species. This conclusion was drawn by Piter (2003). Then, following the results published in Piter et al. (2004a), it is possible to assign a grade of good quality Argentinean *Eucalyptus grandis* to strength class C30, a second one to C24, and the lowest quality one to C18 of the international system established in EN 338 (2009).

3 Results and discussion

3.1 Beam theories and material properties

This section starts with the study of the two well-known Euler–Bernoulli (E–B) and Timoshenko (T) beam theories, and their application to the deflection problem of timber beams. Regarding each one of them, the selection of the material properties is found in the implicit manner. The local MOE (E_{local}) is free of shear effects and it is obtained in the central part of the beam therefore is more representative of the pure bending behavior of the material. This MOE value is applied to the Timoshenko beam theory considering additionally the shear modulus G, which is obtained from the relationship $G = E_{local}/16$, $G = E_{local}/15.94$ and $G = E_{local}/16.07$ according to the relationship established by the norm EN 338 (2009) for strength classes C30, C24 and C18, respectively. The global MOE (E_{global}) includes the zones of the beams under shear effects, thus it is representative of the global stiffness of the beam. This MOE value is applied to the E-B beam theory for the calculation of the mid-span deflection. The analytical deflections were obtained according to the above mentioned assumptions. Beams dimensions and mechanical properties correspond to S4. As a result of the comparison, analytical deflections obtained from the E-B theory with the E_{global} are closer to the experimental results in 70% of the sample. Results of the comparison between experimental outcomes and analytical ones for both theories of the S4 are shown in Fig. 1. Vertical and horizontal axis indicate Timoshenko and Euler Bernoulli deviations regarding the experimental deflections $((v(L/2)_T - v(L/2)_{Exp})$ % and $(v(L/2)_{E-B} - v(L/2)_{Exp})$ %), respectively. The left plot corresponds to visually graded beams and the right plot to mechanical graded beams. As can be observed, the E-B theory shows the best fit and no dependence on the beam quality is observed. This comparison was carried out due to the fact that some standards as the Eurocode 5 (Porteous and Kermani 2007) and the NDS (2005) include the shear deformation for the calculation of deflections but according to the results of this section, the E-B theory adjusts better.

An experimental study of the relationship between the global and local MOE in sawn beams of Argentinean *Eucalyptus grandis* was presented in Piter et al. (2003). This work reports that the local MOE presents a mean value 6–7% larger than the corresponding global one.

It should be noted that although the value of G used in the previous analysis is estimated, not measured, this E_{local}/G relationship is usually employed in the engineering practice. Thus, the source of discrepancy between the numerical and experimental results may be due not only to the selected theory (E–B or T) but also to the G value estimation.

Despite the fact that the E–B theory with the global MOE constant along the beam span has proved its relative accuracy in the prediction of the mid-span deflection of the sample S4, not in all beams the analytical results with the assumption of constant MOE along the span lead to satisfactory outcomes. Therefore, in what follows, an improvement of the prediction of the mid-span deflection based on a stochastic framework is presented.

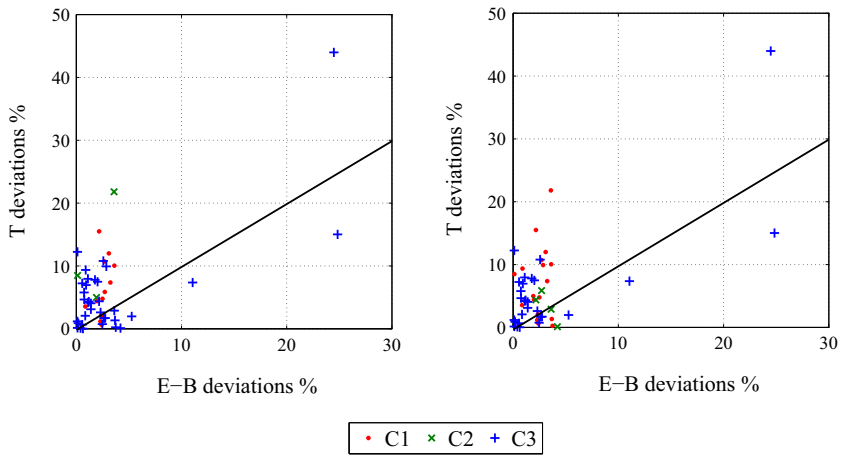

Fig. 1 Percentages differences between the measured deflection of a beam and its corresponding numerical deflection obtained from Euler–Bernoulli and Timoshenko beam theories. *Left plot* beams classified with visual grading, *right plot* same beams classified with machine grading

3.2 Probability density function of the MOE

Firstly, it is necessary to define the PDF of the MOE. To achieve this, the Principle of Maximum Entropy (PME) is employed. It is possible to demonstrate that the application of the principle under the constraints of positiveness due to a real positive domain of the MOE, known first moment and bounded second moment, leads to a gamma PDF.

Second, the Kolmogorov–Smirnov (K–S) test of fit, e.g. Benjamin and Cornell (1970), is applied in order to verify the result of the previous application of the PME. The level of significance α of the parametric hypothesis is assumed to be 0.05. For $\alpha = 0.05$, the critical value for the K–S test of fit is equal to $c = 1.36$. In addition to the gamma distribution, suggested by the PME, the test of fit is also carried out with the log-normal and normal distributions. The first one was selected following Köhler et al. (2007) and the second distribution since it is often employed to represent mechanical properties. The K–S statistics obtained from the test of fit are: 0.63, 0.73 and 0.98 for the gamma, log-normal and normal distributions, respectively. The three distributions fit the K–S test requirements. As can be observed, the gamma distribution fits the experimental data best. However, the use of the normal distribution in the model would occasionally lead to negative values of the MOE. Thus, the gamma and log-normal distribution seem to be more suitable. Also, a truncated normal distribution would be an alternative. Supported by the PME and in view of the test of fit results, the gamma distribution is adopted. The gamma marginal distribution of the MOE is described by the following PDF:

$$f(x \mid a, b) = \frac{1}{b^a \Gamma(a)} x^{a-1} e^{-\frac{x}{b}}, \tag{20}$$

where $a = 28.727$ and $b = 0.44$ are the shape and the scale parameters, respectively and Γ is the Gamma function. The mean value, standard deviation and coefficient of variation of the random variable global MOE are respectively: $\overline{\mu}$ =12.639 GPa, $\overline{\sigma} = 2.358$ GPa and $\delta = \overline{\sigma}/\overline{\mu} = 0.186$. The marginal parameters of the MOE distribution were estimated with the help of the maximum likelihood method (MLM) employing experimental results of the samples presented in Table 1 and reported in Piter (2003).

The selection of the MOE distribution is a point of interest in this work and this fact is easily demonstrated obtaining the percentile 0.05 of the gamma, log-normal and normal distributions with the same mean and standard deviation values. These values of percentile for each distribution are 9.027, 9.165 and 8.76 GPa, respectively and lead to deflections 2.95% (gamma) and 4.45% (log-normal) lower with respect to the 0.05 percentile of the normal one. This value of percentile was chosen due to the fact that it is extensively employed for the design codes in the verification of serviceability conditions. For situations in which a more exhaustive deflections control is required, the 0.05 percentile is recommended by the codes. The comparison among the percentile for different distributions is frequently named as the tail sensitivity problem, e.g. Melchers (1999), and consists in the selection of the best available probabilistic models, in particular those which best model the relevant extreme ('tails') of the PDF.

3.3 Lengthwise variability of the MOE

Two approaches for modeling the lengthwise variability of the MOE are employed and compared. One is the Nataf Transformation (NT) and the other is the Non-Gaussian Karhunen–Loève expansion (NGKL). Both stochastic methods are used in combination with the FEM, resulting in the SFEM. To implement each one of these methods, a discretization technique is necessary. In the first case, the integration point method with nine Gauss-Legendre quadrature points is applied and in the second case, the KLE itself, Eq. (16), yields a discretization technique (Sudret and Der Kiureghian 2000).

It is evident that, if the input is random, the outcomes are also random. In Fig. 2, a convergence study for the random field simulated through the Nataf transformation is shown, where *ns* is the number of independent Monte Carlo simulations, $E[V(L/2)]$ is the mean value of the mid-span deflection and $\sigma[V(L/2)]$ is the standard deviation of the random variable $V(L/2)$. Due to the simple shape of the PDF, the adopted convergence criterion is $|E[V(L/2)_{ns}] - E[V(L/2)_{ns-200}]| \leq 0.05$ mm where $E[V(L/2)_{ns}]$ is the mean value of the mid-span deflection for a number of simulations *ns* and $E[V(L/2)_{ns-200}]$ is the mean value of the mid-span deflection for a number of simulations $ns - 200$. A fast convergence is observed for the mean value and the standard deviation for the studied values of the correlation *d*. This study was carried out in order to determine the appropiate number of simulations to attain a prescribed accuracy taking into account the results that will be shown below.

The first similarities and differences between the two approaches to model the MOE (*i.e.*, either a random variable or a random field) can be observed in Fig. 2. The mean values of $V(L/2)$ remain approximately equal for both approaches. The differences are evident in the standard deviation of $V(L/2)$. The curves of Fig. 2 (right plot) are evidently separated. A correlation length value d_∞ yields larger second moment values (variance). This last observation is the principal difference that the stochastic models exhibit, and the influence on the structural response will be analyzed and discussed in the following subsections.

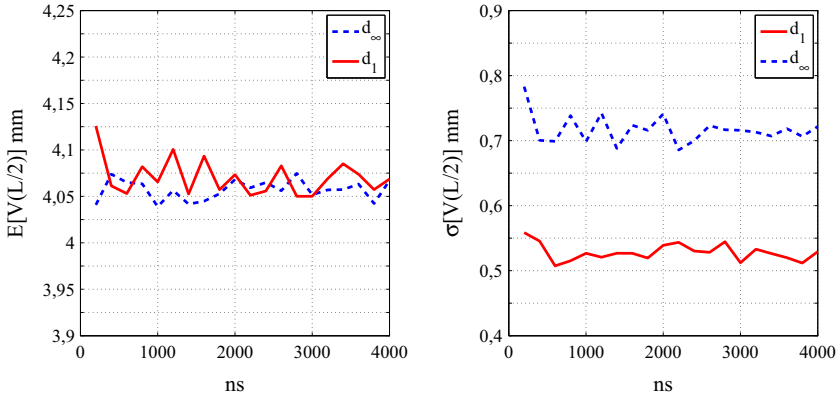

Fig. 2 Convergence of the mean values $E[V(L/2)]$ and the standard deviation $\sigma[V(L/2)]$ for correlation lengths d_1 and d_∞

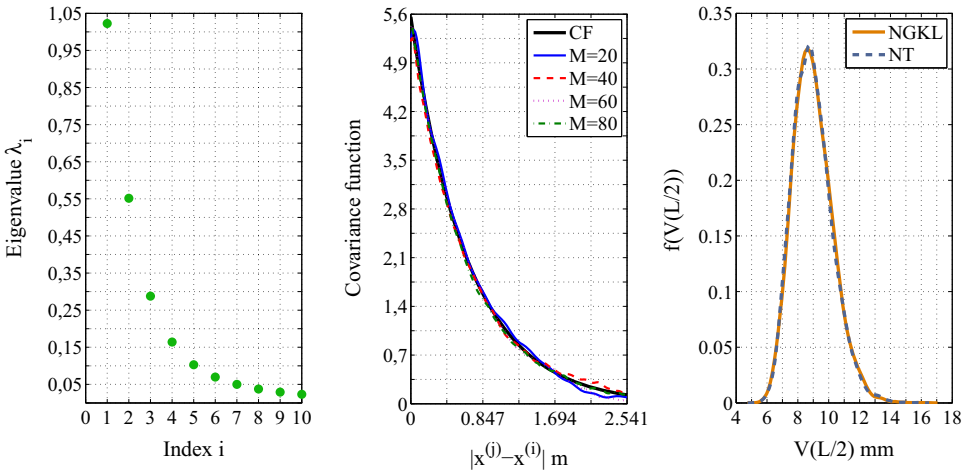

Fig. 3 MOE random field. Comparison of NT and NGKL. *Left plot* first ten eigenvalues of the covariance function. *Central plot* comparison between the prescribed covariance function and the ones obtained for several values of the expansion terms M (number of terms in the NGKL). *Right plot* comparison between the PDF of the mid-span deflection $f(V(L/2))$ obtained for the NGKL and the NT

The application of the NGKL requires the determination of the numbers of terms necessary for an adequate representation of the random field and its properties. Figure 3 depicts the results of this stochastic approach and a comparison with the PDF of the mid-span deflection ($f(V(L/2))$) obtained with the NT. As can be observed in Fig. 3, the approximation of the covariance function (central plot) improves in all points of the beam span for more than 20 terms for the NGKL. The comparison between the PDF of $V(L/2)$ (Fig. 3, right plot) found with the NGKL and the NT shows that both probabilistic tools employed for the simulation of the MOE lengthwise variability conduce to similar results. In Ghanem and Spanos (1991) eigenvalues and eigenfunctions of an exponential covariance function were presented for the KLE. No substantial differences were found although the KL technique exhibits some practical advantages in its implementation.

3.3.1 Numerical validation of the stochastic approach

In this section, a validation of the numerical (stochastic) approach with the experimental results of the mid-span deflection is presented. Experimental data were obtained from the bending test, performed with the samples S2, S3 and S4. These samples were chosen due to the fact that the correlation structure of the random field was determined for beams with similar dimensions to the ones used in this section. Dimensional parameters employed in the numerical simulation are given in Table 3.

Table 3 Dimensional parameters

Parameters	S2	S3	S4
Beam height (mm)	66.48	92.45	141.17
Beam width (mm)	41.89	42.03	41.31
Length between supports (m)	1.196	1.664	2.541
Length between forces (m)	0.398	0.554	0.847

These dimensional parameters correspond to average values obtained from the 50 beams of each sample. The following load values were considered [initial load, (load step), final load]: [0.6, (0.6), 2.4] kN for the sample S2; [0.8, (0.8), 4] kN for the sample S3; [0.9, (0.9), 3.6] kN for 27 beams of the sample S4 and [1.2, (1.2), 2.4] kN for 23 beams of the same sample. The first sub-sample of S4 is composed of: 7 beams C1, 2 beams C2 and 18 C3 beams

visually graded; 9 beams C1, 3 beams C2 and 15 beams C3 according to machine grading. The second sub-sample is composed of: 5 beams C1, 1 beam C2 and 17 beams C3 visually graded; 9 beams C1, 1 beam C2 and 13 beams C3 according to machine grading. Then, the proportion of the beams quality in each sub-sample is similar. No relation between the beam quality and the value of deflection experimentally obtained was observed. Some beams of high quality in samples S2 and S4 have the lowest values of deflection and beams of lower quality the higher values of deflection in S3. But these observations are not conclusive regarding the relationship beam quality-deflection.

The influence of the correlation length can be observed in Fig. 2. The mean values of the response remain approximately equal, for both d_1 and d_∞. An increase of d produces larger standard deviation values of the $f[V(L/2)]$. This indicates that a homogeneous beam presents higher values of deflection than an inhomogeneous beam. Also, a large variation or dispersion from the average or expected value of $V(L/2)$ is observed. In the bending test, the beams are gradually loaded. At the beginning of the test, distortions are frequent before the whole beam starts to bend normally. This behavior is reflected in the load-deformation curve through changes in the slope. As the test progresses, the beam exhibits a linear response and the differences decrease. However, due to the characteristics of the internal structure of the material and the heterogeneities due to the timber defects, the expected straight line is sometimes lost. For this reason, the determination of the global MOE requires the proper selection of the points at the curve so that they are representative of the linear behavior.

In Fig. 4, a comparison of the numerical and experimental CDFs (F) of the mid-span deflection for each sample and load level is presented. Numerical CDFs were obtained with 10,000 MCS. A sensitivity analysis of the correlation length d was carried out and d was considered to range between $3d_1$ and $d_1/2$ with a step of $d_1/4$. In the figures, the numerical mid-span deflection obtained with d_∞, $3d_1$, $d_1/2$ and the value of the correlation length that best fit the experimental results, are depicted. The criterion established for the determination of the correlation length that fits best the experimental results is the quantification of the differences between the numerical and experimental CDF over the entire distribution domain ($\sum \mid F^d - F^{Exp.} \mid$). In Fig. 4a, the CDFs of the mid-span deflection $F(V(L/2))$ for the load levels considered for S2, are compared. In the lower part of the CDF (under 50%), experimental results are located within the numerical CDFs. Deflections for high quality beams (C1 and C2) are found in this region. The numerically found CDF differs from the experimental curve in the upper part of the plot (over 80%). But likewise the lower part of the CDF, deflections of high quality beams are also located in this region. For higher load levels, the probabilistic model with d_1 fits best with the experimental CDF under the percentile 80%. Meanwhile, the numerical model with $3d_1$ fits best the upper part of the experimental CDF (over 80%). Despite this, d_1 achieves the best adjustment in the entire distribution domain.

The CDFs of the mid-span deflection $F(V(L/2))$ for the load levels considered for S3 are compared in Fig. 4b. As can be seen in the upper part of the experimental CDF (over 90%), results are located inside the numerical CDFs range. Meanwhile in the lower part of the CDF (under 30%), numerical results from the probabilistic model with $(3/4)d_1$ and $(1/2)d_1$ are located closer to the experimental ones than the cases included between $(3/4)d_1$ and d_∞. In the central part of the plot (between the 30 and the 80%) the difference among the numerical and experimental CDF is larger. This difference increases with the load level increment. A lack of experimental outcomes exists in this region. It is important to remark that S3 has only 28% of beams of superior quality and constitutes the sample with the lowest amount of this timber quality. But similarly to the previous case, there is no relationship between the timber quality and the experimental mid-span deflection. The model with $(3/4)d_1$ achieves the best representation in the entire distribution domain.

Figure 4c depicts the CDFs of the mid-span deflection $F(V(L/2))$ found with the load levels considered for S4. The CDF obtained from the probabilistic model with $(5/4)d_1$ fits best with the experimental one for all the load levels and the two sub-samples. For $(1/2)d_1$ the first sub-sample of experimental results is best adjusted over the percentile 80%. But the improvement achieved with $(5/4)d_1$ in both sub-samples is highest. Also, the proportion of beam quality in each sub-sample is similar. The model with d_∞ tends to overestimate the lower values of deflections and underestimate the higher values. Unlike the previous sample, the experimental mid-span deflections of high quality beams are located in the lower part of the experimental CDF (under 50%) for the higher load steps. The model with $(5/4)d_1$ is the best fit in the entire distribution domain.

Results of the sensitivity analysis show that the numerical outcomes obtained with d_1 are, on average, acceptable and result in a good prediction of mid-span deflection of the tested sample. The value of the correlation length for a serviceability load level obtained from pine-spruce samples is applicable to *Eucalyptus grandis* structural elements. Although values of $(3/4)d_1$ and $(5/4)d_1$ have shown the better adjustment in the mid-span distribution for S3 and S4 respectively, d_1 appears to be a reasonable value for the whole study. The statistical information of the MOE embodied in its PDF constitutes a solid base from which the structural designer can obtain the

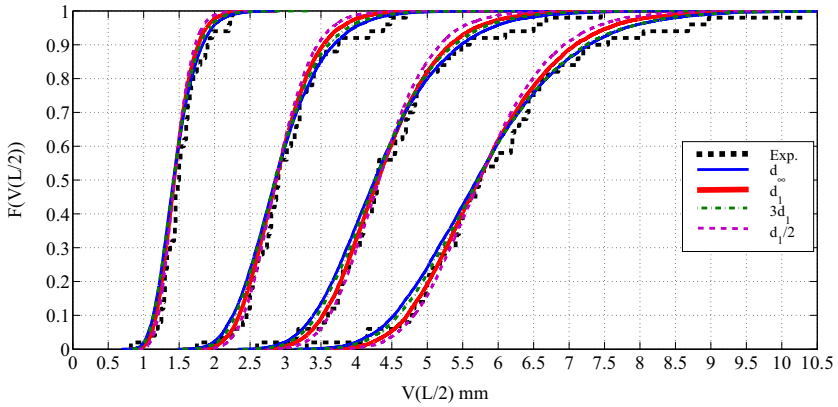

(a) Sample S2 load values [0.6, (0.6), 2.4] kN. Best fit with $d = d_1$.

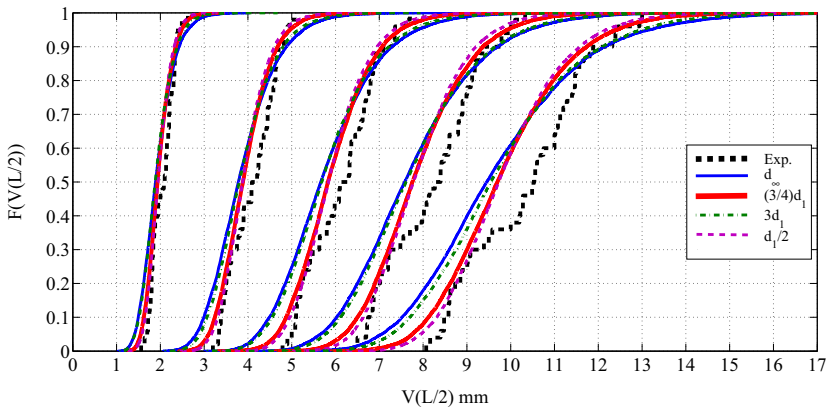

(b) Sample S3 load values [0.8, (0.8), 4] kN. Best fit with $d = (3/4)d_1$.

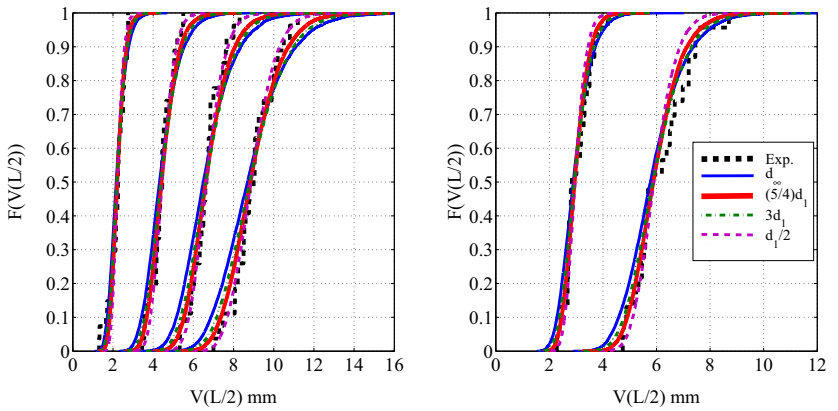

(c) Sample S4a load values [0.9, (0.9), 3.6] kN left plot. Sample S4b [1.2, (1.2), 2.4] kN right plot. Best fit with $d = (5/4)d_1$.

Fig. 4 Comparison between numerical and experimental CDFs. Sensitivity analysis of the correlation length parameter d

structural response. Results of the numerical approximation of the mid-span deflections for both models of MOE variation (d_∞ and d) are presented and compared in Table 4. Differences between the results of the model with d_∞ and the experimental values are presented in the seventh column of the table ($F^{d_\infty} - F^{Exp.}$). Similarly, for the values of the correlation length that best fit the experimental CDFs ($F^{d} - F^{Exp.}$) in the eighth column. Also, the mean value, standard deviation (SD), the 5th and 95th percentile (P05 and P95, respectively) are presented in the table. As can be observed, the predictability of the experimental results increases with the application of the numerical model that includes the lengthwise variability of the MOE, named F^d, in all the samples and load levels.

Table 4 Differences in the predictability of the experimental results obtained by numerical models (d_∞ and d)

Sample	Load (kN)	Statistics (mm)	Exp.	d_∞	d	$F^{d_\infty} - F^{Exp.}$ (%)	$F^{d} - F^{Exp.}$ (%)
S2 $d = d_1$	0.6	Mean	1.52	1.45	1.45	10.41	8.64
		SD	0.28	0.27	0.24		
		P05	1.18	1.07	1.14		
		P95	2.08	1.95	1.89		
	1.2	Mean	3.01	2.92	2.91	7.39	5.2
		SD	0.58	0.56	0.47		
		P05	2.31	2.12	2.23		
		P95	4.28	3.97	3.77		
	1.8	Mean	4.47	4.36	4.38	5.45	3.95
		SD	0.89	0.84	0.72		
		P05	3.34	3.19	3.34		
		P95	6.32	5.91	5.68		
	2.4	Mean	5.97	5.82	5.83	6.01	4.15
		SD	1.25	1.10	0.95		
		P05	4.37	4.26	4.46		
		P95	8.39	7.79	7.55		
S3 $d = (3/4)d_1$	0.8	Mean	2.05	1.93	1.97	27.78	13.10
		SD	0.25	0.37	0.28		
		P05	1.70	1.41	1.56		
		P95	2.39	2.63	2.47		
	1.6	Mean	4.08	3.88	3.87	27.11	6.28
		SD	0.52	0.76	0.60		
		P05	3.34	2.82	3.15		
		P95	4.87	5.27	4.95		
	2.4	Mean	6.11	5.91	5.92	33.08	5.73
		SD	0.78	1.13	0.86		
		P05	5.02	4.21	4.66		
		P95	7.34	7.87	7.43		
	3.2	Mean	8.18	7.85	7.87	32.15	6.23
		SD	1.05	1.47	1.14		
		P05	6.70	5.66	6.20		
		P95	9.90	10.40	9.91		
	4	Mean	10.33	9.81	9.84	31.16	7.58
		SD	1.36	1.89	1.42		
		P05	8.43	7.05	7.76		
		P95	12.42	13.17	12.43		
S4 $d = (5/4)d_1$	0.9	Mean	2.21	2.21	2.24	4.90	4.48
		SD	0.38	0.42	0.34		
		P05	1.42	1.59	1.74		
		P95	2.73	2.99	2.84		
	1.8	Mean	4.43	4.42	4.47	6.63	2.98
		SD	0.55	0.85	0.68		
		P05	3.56	3.20	3.51		
		P95	5.34	5.98	5.69		
	2.7	Mean	6.66	6.65	6.72	9.95	3.19
		SD	0.75	1.29	1.01		
		P05	5.42	4.84	5.27		
		P95	7.89	9.02	8.55		

Table 4 continued

Sample	Load (kN)	Statistics (mm)	Exp.	d_∞	d	$F^{d_\infty} - F^{Exp.}$ (%)	$F^{d} - F^{Exp.}$ (%)
	3.6	Mean	8.99	8.88	8.97	10.17	3.83
		SD	1.04	1.69	1.34		
		P05	7.33	6.50	7.02		
		P95	10.71	11.95	11.37		
	1.2	Mean	3.03	2.96	2.98	4.17	2.58
		SD	0.49	0.58	0.44		
		P05	2.38	2.14	2.33		
		P95	3.77	4.02	3.76		
	2.4	Mean	6.15	5.92	5.98	5.79	2.66
		SD	1.02	1.14	0.90		
		P05	4.78	4.32	4.68		
		P95	7.49	7.95	7.58		

3.4 Effects of the lengthwise variability of MOE on the reliability of timber beams

The comparison between experimental and numerical results obtained from the probabilistic model that take into account the lengthwise variability of the MOE in timber elements has been discussed previously. In this subsection, a study regarding the performance of structural-sized beams of Argentinean *Eucalyptus grandis* is presented and discussed in comparison with the deflection limits recommended by the Argentinean design rules (CIRSOC 601 2013).

3.4.1 Beams with MOE represented by a random variable

The serviceability limit state function for a simply supported beam can be expressed as:

$$g(E) = w_R - w_m(E), \tag{21}$$

where w_R is the deterministic allowable deflection (reference value) assumed in accordance with the functional requirement and $w_m(E)$ is the random mid-span deflection. Taking into account the instantaneous mid-span deflection caused by the load configuration considered in this work, the serviceability limit state function can be expressed as:

$$g(E) = \frac{L}{360} - \frac{p}{Ei}\frac{23L^3}{648}, \tag{22}$$

where L is the beam length, the first term is the expression applied to the verification of the instantaneous deflection due to actions according to the criterion adopted by the Argentinean design rules (CIRSOC 601 2013) and the second term is the random mid-span deflection. Following this standard, the instantaneous deflection can be calculated using the mean value or the percentile 0.05 of the MOE distribution, depending on the design situation. For more critical design situations in which a more exhaustive deflections control is required, the 0.05 percentile is recommended by the codes. The probability of exceeding the serviceability condition, i.e. the probability that the random mid-span deflection be greater than the allowable one is defined as:

$$PF = P(g(E) \leq 0) = \int_{g(E)\leq 0} f_E(e)de, \tag{23}$$

in which f_E is the PDF of the random variable E. This expression is relatively simple to solve in the case of $d \to \infty$, i.e. MOE with homogeneous value within the beam length. It is only necessary to solve the limit state function when $g(E) = 0$ in order to find the value of the dependent variable, say loads, cross sectional dimensions, beam length. For values of $g(E) \leq 0$ the failure occurs, i.e. the violation of the allowable deflection requirement.

Let us take into account the dimensional parameters of the sample S4 and the following *Eucalyptus grandis* material properties, corresponding to the C1 strength class: $\overline{\mu}$ =13.902 GPa and $\overline{\sigma}$ = 2.364 GPa. If one previously defines a target value of *PF*, the load values that produce this probability of exceeding the serviceability performance condition can be found. For a *PF* equal to 0.05, the obtained load value is 1.33 kN and for a *PF* equal to 0.1, 1.43 kN. These load values were verified to be within the linear elastic range of the material and within the load magnitudes that have been employed in the bending tests.

When the lengthwise variability of the MOE is considered in the calculations, the study concerning the serviceability control leads to a lower *PF* for lower load levels. Additionally, a higher *PF* results for load levels closer to the bending capacity of the beams, always in comparison with the constant MOE assumption. This point will be discussed in the following subsection. When the properties are considered

constant along the structural element the design criteria (percentile 0.05 of the MOE distribution) are found to be on the safe side.

3.4.2 *Beams with lengthwise MOE variability represented by a random field*

In this section, the PF is approximated by the Monte Carlo Method (MCM, Melchers 1999) for the load values previously determined and the MOE is represented by a random field with correlation length d_1. The MCM is chosen due to the fact that f_E (Eq. (23)) becomes a multidimensional PDF (a random field) in this section and the limit state function is not straightforward defined as before. This method provides a simple technique in order to estimate the probability of failure PF. The confidence interval of PF is defined as follows:

$$P\left(\widehat{PF} - z_{1-\alpha/2}\frac{S}{\sqrt{N}} \le PF \le \widehat{PF} + z_{1-\alpha/2}\frac{S}{\sqrt{N}}\right) \approx 1-\alpha, \tag{24}$$

where $z_{1-\alpha/2}$ is the $(1-\alpha/2)$ quantile of the standard normal distribution, $\widehat{PF}$ is the unbiased estimator of PF and S is its variance. The relative error (RE) of the estimator $\widehat{PF}$ with N simulations is defined as

$$RE = \frac{\sqrt{Var(\widehat{PF})}}{E[\widehat{PF}]} = \frac{\sigma}{PF\sqrt{N}} \approx \frac{S}{\widehat{PF}\sqrt{N}}. \tag{25}$$

The probability of exceeding the limit value of the instantaneous deflection decreases when the lengthwise variability of the MOE is considered, as shown in Table 5. Also, a probability of failure equal to approximately 0.05 can be achieved for the stochastic model with d_1 while its corresponding case with $d \to \infty$ has a probability of failure equal to 0.1. Next, in the same table, the RE of the estimator $\widehat{PF}$ and the confidence interval for a probability of 0.95 with a number of simulations N=100,000 are shown. The relative error reported in the table shows the accuracy of the estimator $\widehat{PF}$.

Figure 5 depicts the results of the reliability study. The variation of the estimator $\widehat{PF}$ with its relative error and the confidence interval for the corresponding PF in the models when $d \to \infty$, are shown. The relative error of $\widehat{PF}$ is lower in the case $d \to \infty$ and $PF = 0.1$ due to the reduction of the ratio between the standard deviation of the estimator and its value with respect to the case $d \to \infty$ and $PF = 0.05$. Additionally, the decrease of the absolute width of the confidence interval with respect to the increment of N is observed. The difference in the values of these parameters is due to the variation of the standard deviation of $\widehat{PF}$ that decreases with the increment of $\widehat{PF}$.

Table 5 $\widehat{PF}$ estimator, its relative error (RE) (% of $\widehat{PF}$) and the confidence interval of PF. $N = 100{,}000$

$PF_{d\to\infty}$	$\hat{PF}_{d_1}$	RE	Confidence interval 95%	
			Lower limit	Upper limit
0.05	0.0173	2.37	0.0165	0.0181
0.10	0.0515	1.35	0.0501	0.0529

There exists variability in the mechanical properties within each strength class established by the norms. The visual strength grading parameters reduce this variability with respect to the total population. The designer takes the properties of the strength class and applies them to the calculation of the whole piece without considering (within the established limits) that the defects and properties vary along the same piece. Following the calculation criterion considered in the Argentinean standard CIRSOC 601 (2013) without taking into account its lengthwise variability, a $PF = 0.05$ is assumed, i.e. there exists a probability of 0.05 that the MOE takes a smaller value. According to the results of the present study, the probability of exceeding the serviceability condition is lower in the presence of a lengthwise variable MOE than when the usual calculation rules are applied.

The preceding observations are important for the practical design of timber elements that adopt a failure probability of 0.05. The influence of the lengthwise variability of the MOE in the serviceability performance for several load values can be appreciated in a fragility curve. Figure 6 shows the fragility curves of the samples S2, S3 and S4 for the load levels applied in the experimental test. They were constructed through the calculation of the PF for each load level. As can be observed for lower load levels, the PF is lower when there is lengthwise variability of the MOE and vice versa for higher load levels. Then, the importance of a more precise deflection prediction is apparent. Another relevant point is that for these load levels, failure for the bending strength of the beams were not registered during the experimental test. This fact shows the importance of the serviceability performance in the structural design and of a more realistic prediction of the mid-span deflection.

4 Conclusion

Structural-sized beams of Argentinean *Eucalyptus grandis* with uncertain material properties were studied and in particular, the mid-span deflection was analyzed in detail. A stochastic model of the lengthwise variability of the

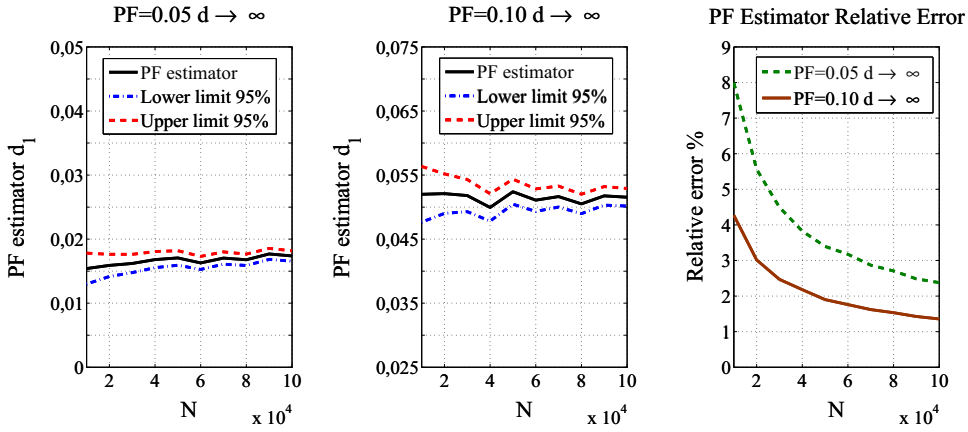

Fig. 5 Estimator of the probability of failure ($\hat{PF}$) and its respective relative error for a $PF = 0.05$ and 0.1 of beams with a constant MOE

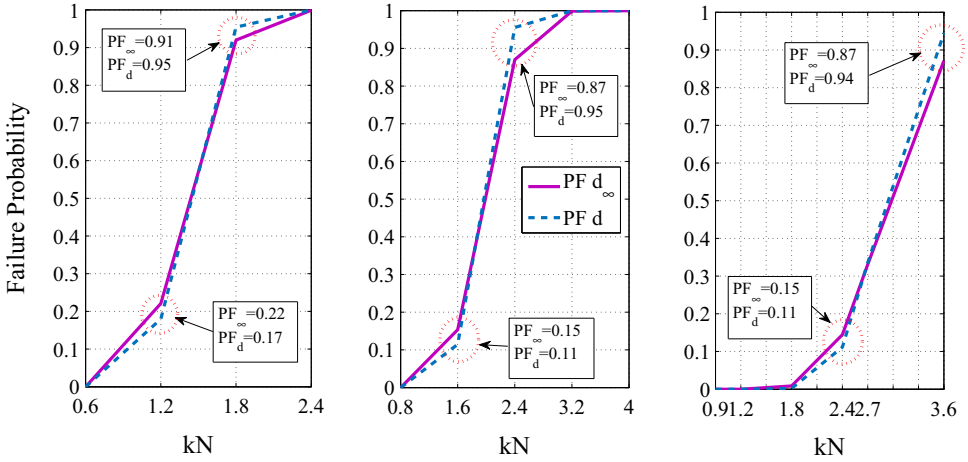

Fig. 6 Fragility curves for the samples S2 ($d = d_1$), S3 ($d = (3/4)d_1$) and S4 ($d = (5/4)d_1$) from *left* to *right*. Numerical results

Modulus of Elasticity (MOE) that improves the predictability of the structural response was proposed.

The model relies on experimental values of the MOE obtained with third-point load bending tests. Usually, the MOE lengthwise distribution is not known. The present methodology has shown that, despite this situation, numerical results fit very satisfactorily the experimental data. The bending moment distribution along the length of the beams, and the maximum values, are similar to those produced by a uniform load. This type of load is more frequent in structures. Beam dimensions of each sample are representative of the elements used in the usual timber structures. Pieces with a height higher than 150 mm are not usually available because of the relatively small diameter of the stems which are normally obtained from short rotation plantation trees. These two facts, load configuration of the bending test and beam dimensions, support the eventual extension of the results presented in the work.

The development of the numerical model involves the following steps: first, the distribution of the global MOE was chosen based on the Principle of Maximum Entropy (PME). Then, the selection was verified with the Kolmogorov–Smirnov (K–S) test of fit. The results of the application of these two tools have shown that the best Probability Density Function (PDF) to model the MOE is the gamma PDF instead of the extensively employed normal PDF. Then, the Euler–Bernoulli beam model with the application of the global MOE has proved to be more accurate in the prediction of the deflections of structural size beams than the Timoshenko beam model that employs the local MOE and the shear modulus. However, the source of discrepancy between numerical and experimental results can be due not only to the selected beam theory but also to the shear modulus estimation usually employed in the engineering practice. The structure of correlation of the random field was adopted and estimative values of the correlation length were established, supported by the mechanical similarities that the Argentinean *Eucalyptus grandis* shows with respect to coniferous species. Finally, two approaches were employed and compared in order to simulate the lengthwise variability of the MOE within a Stochastic Finite Element Method (SFEM) code. The applicability of the non-Gaussian Karhunen–Loève

expansion (NGKL) and the Nataf Transformation (NT) was discussed and it was found that both tools lead to similar results. The first approach is recommended due to its practical implementation advantages.

Experimental values of the mid-span deflection obtained from the bending test were evaluated and classified according to the visual and machine grading of the tested beams. Results of the machine grading were used in order to improve the study of the deflections measured in each sample. The first grading method is applicable under the Argentinean design code. The machine grading does no result in decisive considerations regarding the beams deflections. No relation between the beams quality and the deflection was observed.

Validation of numerical results of bending tests with experimental ones was also presented. It is shown that numerical simulations results with the MOE represented by a random field, are closer to the experimental outcomes. Thus, an improvement of the deflection predictability with respect to the constant MOE assumption was achieved. The value of the correlation length for a serviceability load level obtained from pine-spruce beams was shown to be applicable to *Eucalyptus grandis* elements. Results of a sensitive study shows that the highest adjustment in the mid-span deflection prediction was achieved with values of correlation length closer to the adopted reference value.

Finally, the Monte Carlo Method (MCM) was applied to the study of the serviceability performance of timber beams through the stochastic model presented in this work. When the lengthwise variability of MOE is considered, the probability of exceeding the serviceability limit is lower compared with the use of a constant MOE along the beam span. This fact is true for low values of the Probability of Failure(*PF*). According to the results provided by the model of lengthwise variability of the MOE for a probability of failure of 0.05, a model with constant MOE should be employed considering the 0.1 percentile of the MOE distribution. This is an important point regarding the Serviceability Limit State (SLS) design of *Eucalyptus grandis* timber elements. In order to study the influence of the lengthwise variability of the MOE for several loads in the structural performance, the fragility curves of the tested beams were obtained. For higher values of the *PF*, the probability of exceeding the serviceability limit is higher for a model with lengthwise variability of the MOE. The findings of this study show the importance of the serviceability design. The serviceability limit is the first condition reached while the bending strength failure is far for the tested samples. Despite this fact, the stochastic model herein presented has no influence on the Ultimate Limit State (ULS) design of *Eucalyptus grandis* timber elements if a first order beam theory is used. Hence, in the case herein analyzed, one can infer that the stochastic approach that takes into account the lengthwise variability of the MOE leads to a more precise prediction of the serviceability performance than the model with constant MOE along the beam span.

Acknowledgements This study was partially supported by CONICET and SGCyT-UNS. The experimental data provided by J. C. Piter and co-workers from FRCU-UTN (Argentina) is greatly acknowledged by the authors.

References

ASTM D 198 (2002) Standard test methods of static tests of lumber in structural sizes. American Society for Testing and Materials (ASTM), West Conshohocken, United States

Bathe KJ (1982) Finite element procedures in engineering analysis. Prentice-Hall, New Jersey

Benjamin RJ, Cornell CA (1970) Probability, statistics and decision for civil engineers. McGraw-Hill, New York

Brandner R (2012) Stochastic system actions and effects in engineered timber products and structures. PhD thesis, Graz University of Technology

Brandner R, Schickhofer G (2015) Probabilistic models for the modulus of elasticity and shear in serial and parallel acting timber elements. Wood Sci Technol 49(1):121–146

CIRSOC 601 (2013) Argentinean standard of timber structures (In Spanish). Instituto Nacional de Tecnología Industrial (INTI)-Centro de Investigación de los Reglamentos Nacionales de Seguridad para las Obras Civiles (CIRSOC), Buenos Aires

Czmoch I (1998) Influence of structural timber variability on reliability and damage tolerance of timber beams. PhD thesis, Luleå Tekniska Universitet, Luleå

Der Kiureghian A, Ke JB (1988) The stochastic finite element method in structural reliability. Probab Eng Mech 3(2):83–91

Der Kiureghian A, Liu PL (1986) Structural reliability under incomplete probability information. J Eng Mech-ASCE 112:85–104

Ditlevsen O, Källsner B (2005) Span-dependent distributions of the bending strength of spruce timber. J Eng Mech-ASCE 131(5):485–499

EN 338 (2009) Structural timber. Strength classes; German version. European Committee for Standardization (CEN). DIN Deutsches Institut fr Normung e. V., Berlin

EN 384 (1996) Structural timber. Determination of characteristic values of mechanical properties and density (in Spanish). AENOR-Asociación Española de Normalización y Certificación, Madrid

EN 408 (1996) Timber structures. Structural timber and glued laminated timber. Determination of some physical and mechanical properties (in Spanish). AENOR-Asociación Española de Normalización y Certificación, Madrid

Fink G, Köhler J (2014) Model for the prediction of the tensile strength and tensile stiffness of knot clusters within structural timber. Eur J Wood Prod 72(3):331–341

García D, Sampaio R, Rosales M (2016) Eigenproblems in timber structural elements with uncertain properties. Wood Sci Technol. doi:10.1007/s00226-016-0810-8

Ghanem RG, Spanos PD (1991) Stochastic finite elements: a spectral approach. Springer, New York

IRAM 9662-2 (2006) Glued laminated timber. Visual strength grading of boards, part 2: boards of Eucalyptus grandis (in Spanish). Argentinean Institute for Standardization and Certification (IRAM), Buenos Aires

Isaksson T (1999) Modeling the variability of bending strength in structural timber: length and load configuration effects. PhD thesis, Lund Institute of Technology, Lund

Jaynes E (1957) Information theory and statistical mechanics. Phys Rev 106(4):620–630

Kandler G, Füssl J, Eberhardsteiner J (2015a) Stochastic finite element approaches for wood-based products: theoretical framework and review of methods. Wood Sci Technol 49(5):1055–1097

Kandler G, Füssl J, Serrano E, Eberhardsteiner J (2015b) Effective stiffness prediction of glt beams based on stiffness distributions of individual lamellas. Wood Sci Technol 49(6):1101–1121

Kline DE, Woeste FE, Bendtsen B (1986) Stochastic model for modulus of elasticity of lumber. Wood Fiber Sci 18(2):228–238

Köhler J (2007) Reliability of timber structures. PhD thesis, Swiss Federal Institute of Technology, Zürich

Köhler J, Sørensen JD, Faber MH (2007) Probabilistic modeling of timber structures. Struct Saf 29(4):255–267

Lam F, Varoğlu E (1991) Variation of tensile strength along the length of lumber. Part 2: Model development and verification. Wood Sci Technol 25(6):449–458

Melchers RE (1999) Structural reliability: analysis and prediction. Wiley, New York

Mulani S (2006) Uncertainty quantification in dynamic problems with large uncertainties. PhD thesis, Virginia Polytechnic Institute and State University, Blacksburg

NDS (2005) National Design Specification for Wood Construction. American Forest & Paper Association (AF&PA)—American Wood Council (AWC)

Piter J (2003) Strength grading of sawn timber as structural material: development of a method for the Argentinean Eucalyptus grandis (in Spanish). PhD thesis, Universidad Nacional de la Plata, La Plata

Piter J, Zerbino R, Blaß H (2003) Relationship between global and local modulus of elasticity in beams of argentinean eucalyptus grandis. Maderas Ciencia y Tecnología 5(2):107–116

Piter J, Zerbino R, Blaß H (2004a) Visual strength grading of Argentinean Eucalyptus grandis. Holz Roh Werkst 62(1):1–8

Piter J, Zerbino R, Blaß H (2004b) Machine strength grading of argentinean eucalyptus grandis: main grading parameters and analysis of strength profiles according to european standards. Holz Roh Werkst 62(1):9–15

Porteous J, Kermani A (2007) Structural timber design to Eurocode 5. Wiley

SBN 1980 (1981) Swedish Building Code (in Swedish). National Swedish Board of Physical Planning and Building, Stockholm

Shannon C (1948) A mathematical theory of communication. Bell Sys Technol J 27:379–423

Sudret B, Der Kiureghian A (2000) Stochastic finite element methods and reliability: a state-of-the-art report. Department of Civil and Environmental Engineering, University of California

Wang Y, Foschi R (1992) Random field stiffness properties and reliability of laminated wood beams. Struct Saf 11(3–4):191–202